Journal of Nondestructive Evaluation, Vol. 25, No. 1, March 2006 (© 2006)
DOI: 10.1007/s10921-006-0004-7

Acoustic Nonlinearity Parameter Due to Microplasticity

J.-Y. Kim,[1] J. Qu,[1,3] L. J. Jacobs,[1] J. W. Littles,[2] and M. F. Savage[2]

Received 27/10/05; Revised 1/2/06; Publishe online: 5/26/06

Acoustic nonlinearity (which is quantified in terms of an absolute material parameter, the acoustic nonlinearity parameter, β) can be caused by several sources, one of which is the elastic-plastic deformation of the material. This paper develops a model to quantify the acoustic nonlinearity parameter due to elastic-plastic deformation. This new model is applicable to general anisotropic elastic-plastic materials with existing Microplasticity strains due to either monotonic or cyclic loading. As an example, the developed model is applied to calculate the acoustic nonlinearity parameter of a single crystal copper specimen subjected to cyclic fatigue loading. It is found that the acoustic nonlinearity parameter of this specimen increases monotonically with increasing fatigue cycles.

KEY WORDS: Acoustic nonlinearity; nonlinear ultrasonic measurement; plasticity; single crystal plasticity; dislocations.

1. INTRODUCTION

Ultrasonic techniques have been used extensively for nondestructiveevaluation and inspection of engineering components and structures. However, linear ultrasonic techniques are typically limited to the detection of flaws such as cracks and delaminations. For material property characterization, linear ultrasonic methods are primarily used to measure elastic properties and attenuation characteristics. Recent developments in the physics-based diagnosis and prognosis of aerospace structural systems represent a great opportunity (and need) for nondestructive methods that are capable of assessing fatigue damage accumulation in critical components in the early stages of fatigue life, before the formation of any macroscopic cracks. One candidate method that has the potential to nondestructively characterize damage accumulation at such a micro-structural level is nonlinear ultrasonics.

When elastic waves propagate through a nonlinear medium, higher order harmonics are generated.[1] The magnitude of one of these harmonics, the second order harmonic, gives a direct measure of the acoustic nonlinearity parameter (β), an absolute non-dimensional parameter that characterizes the nonlinearity of the medium. It has been shown experimentally[2–5] that there is a very good correlation between the fatigue damage and the acoustic nonlinearity parameter in metallic materials. The early work of Suzuki et al.[2] and Hikata et al.[3] found that the measured acoustic nonlinearity parameter in plastically deformed single crystal aluminum was much higher than what the lattice anharmonicity can possibly generate. They attributed such an increase in the acoustic nonlinearity parameter to dislocation glide. Using the Granato-Lucke dislocation string model[6] for pinned dislocations, they found a qualitative correlation between dislocation density and the acoustic nonlinearity parameter. Morris et al.[5] applied the acoustic nonlinearity measurement technique to

[1] G. W. Woodruff School of Mechanical Engineering, Georgia Institute of Technology, Atlanta, GA 30332-0405, USA.
[2] Pratt & Whitney Materials & Processes Engineering, 400 Main Street, M/S 114-40 East Hartford, CT 06108.
[3] Corresponding author: E-mail: jianmin.qu@me.gatech.edu

evaluate fatigue damage of Al-7075-T6 alloy. They attributed the increase of acoustic nonlinearity to the microcracks on the surface. Cantrell and Yost[7] found that the contribution of dislocation dipoles is even more significant in polycrystalline materials since the monopole loop lengths in these materials are usually much shorter than the ones used for the calculations in earlier investigations. More recently, Cantrell[8] proposed a model in which the evolution of sub-structural organization of dislocations is taken into account to predict total acoustic nonlinearity of a polycrystalline nickel under cyclic load. Application of Cantrell's model to aluminum alloy 2024-T4 under fatigue loading yields excellent agreement between theory and experiment.[9]

Although Cantrell's dislocation-based model provides a quantitative relationship between dislocation density and the acoustic nonlinearity parameter, this model requires detailed information about the dislocation sub-structure, such as the dislocation loop length and dipole height. To be predictive, this model also requires the evolution of statistical parameters such as the densities of dislocation monopoles and dipoles, and the volume fractions of vein and persistent slip bands (PSBs) during the fatigue. In practice, however, most of these parameters are not easily measured experimentally, nor can they be accurately predicted with current modeling capabilities; this is especially true when considering the evolution of these parameters during fatigue.

In this paper, we propose an alternative approach to predict the acoustic nonlinearity parameter. Instead of relating the acoustic nonlinearity parameter directly to the dislocation sub-structure (and its evolution), we instead consider the continuum manifestation of these dislocations, namely, plastic deformation. It is well known that plastic deformation in metallic materials is a consequence of dislocation dynamics. Therefore, it is conceivable that there is a correlation between dislocation density and the amount of plastic deformation in a given sample. The advantage of formulating the acoustic nonlinearity parameter in terms of the amount of plastic strain in a material is that plastic strain is a macroscopic and phenomenological parameter that quantitatively characterizes the affect of the dislocation substructure. Therefore, the prediction of plastic strain and its accumulation during fatigue does not require detailed information on dislocation substructures. The evolution of cumulative plastic strain for crystalline metals has been extensively studied using crystal-plasticity theories. Since the plastic strain and its evolution can be simulated with sufficient accuracy and efficiency, a model that relates the acoustic nonlinearity parameter to the cumulative plastic strain has the potential to predict the relationship between the acoustic nonlinearity parameter and the fatigue life of a component. This direct linkage will enable the nondestructive evaluation of the remaining fatigue life of a component by measuring the component's acoustic nonlinearity parameter.

2. WAVE PROPAGATION IN A MEDIUM WITH INITIAL MICROPLASTICITY

To develop the model, we introduce three material states: the natural, the initial and the current configuration.[10] The natural configuration describes the virgin state of the material when it is free from any deformation and stresses. The initial configuration refers to the material state when certain microplasticity had occurred in the material, while the current configuration denotes the material state with ultrasonic wave-induced dynamic deformation superimposed on the initial state of the material. In our analysis, the deformation from the current to the initial states (due to ultrasonic wave motion) is assumed small, but the deformation from the natural state to the initial state can be finite. Furthermore, the deformation from the natural state to the initial state is assumed known.

We will denote the field quantities in the initial and current states with superscripts i and c, respectively. As shown in Fig. 1, the location of a material particle in the natural, initial and current states are denoted by the position vectors $\boldsymbol{\xi}$, $\mathbf{X}$, and $\mathbf{x}$, all from the origin of a common Cartesian reference coordinate system. The displacement of material particles

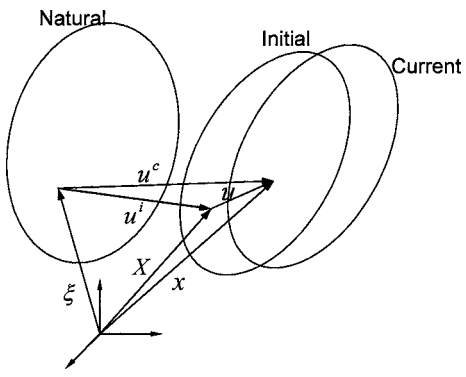

Fig. 1. Three material configurations: natural (ξ), initial (X) and current (x).

from the natural to the initial, and from the natural to the current states can be thus written, respectively, as

$$\mathbf{u}^i = \mathbf{X} - \boldsymbol{\xi}, \qquad \mathbf{u}^c = \mathbf{x} - \boldsymbol{\xi}. \tag{1}$$

It thus follows that the wave motion is described by

$$\mathbf{u} = \mathbf{u}^c - \mathbf{u}^i = \mathbf{x} - \mathbf{X}. \tag{2}$$

The deformation from the natural state to the initial state can be fully characterized by the deformation gradient tensor,

$$F_{I\alpha} = \frac{\partial X_I}{\partial \xi_\alpha} = \frac{\partial u_I^i}{\partial \xi_\alpha} + \delta_{I\alpha}. \tag{3}$$

Since the ultrasonic wave motion is considered as a small disturbance from the initial state, we may use the small strain

$$\varepsilon_{\alpha\beta} = \frac{1}{2}\left(\frac{\partial u_\alpha}{\partial \xi_\beta} + \frac{\partial u_\beta}{\partial \xi_\alpha}\right) \tag{4}$$

to measure the deformation from the initial state to the current state, i.e., we assume

$$\left(\frac{\partial u_\lambda}{\partial \xi_\alpha}\right)^2 \approx 0. \tag{5}$$

To describe the deformation from the natural state to the initial state, we use the Lagrangian strain measure,

$$E^i_{\alpha\beta} = \frac{1}{2}\left(\frac{\partial u^i_\alpha}{\partial \xi_\beta} + \frac{\partial u^i_\beta}{\partial \xi_\alpha} + \frac{\partial u^i_\lambda}{\partial \xi_\alpha}\frac{\partial u^i_\lambda}{\partial \xi_\beta}\right) \tag{6}$$

where, and in the rest of this paper, repeated index means summation from 1 to 3. Similarly, the Lagrangian strain tensor from the natural to the current state is given by

$$E^c_{\alpha\beta} = \frac{1}{2}\left(\frac{\partial u^c_\alpha}{\partial \xi_\beta} + \frac{\partial u^c_\beta}{\partial \xi_\alpha} + \frac{\partial u^c_\lambda}{\partial \xi_\alpha}\frac{\partial u^c_\lambda}{\partial \xi_\beta}\right). \tag{7}$$

The difference between these two strain tensors can be written as

$$\begin{aligned} E_{\alpha\beta} &= E^c_{\alpha\beta} - E^i_{\alpha\beta} \\ &= \frac{1}{2}F_{I\alpha}F_{J_\beta}\left(\frac{\partial u_I}{\partial X_J} + \frac{\partial u_J}{\partial X_I} + \frac{\partial u_K}{\partial X_I}\frac{\partial u_K}{\partial X_J}\right). \end{aligned} \tag{8}$$

In deriving (8), we have made use of (1)–(2). Note that this difference in the strain tensors is not the same small strain defined in (4). For future use, we write (8) in an alternative form,

$$E_{\alpha\beta} = A_{\alpha\beta IJ}\left(\frac{\partial u_I}{\partial X_J} + \frac{1}{2}\frac{\partial u_K}{\partial X_I}\frac{\partial u_K}{\partial X_J}\right), \tag{9}$$

where

$$A_{\alpha\beta IJ} = \frac{1}{2}(F_{I\alpha}F_{J\beta} + F_{J\alpha}F_{I\beta}). \tag{10}$$

Now, let $\tilde{\sigma}^i_{\alpha\beta}$ be the second Piola-Kirchhoff[11,12] stress of the initial state written in the natural configuration, and $\tilde{\sigma}^c_{\alpha\beta}$ be the second Piola-Kirchhoff stress of the current state written in the natural configuration. Then, the stress increment from the initial state to the current state due to ultrasonic wave motions (written in the natural configuration) is given by

$$\tilde{\sigma}_{\alpha\beta} = \tilde{\sigma}^c_{\alpha\beta} - \tilde{\sigma}^i_{\alpha\beta}. \tag{11}$$

Written in the initial configuration, the same stress increment can be expressed as[10,11],

$$\tilde{\sigma}_{IJ} = \frac{1}{J}F_{I\alpha}F_{J\beta}\tilde{\sigma}_{\alpha\beta} = \frac{1}{J}A_{\alpha\beta IJ}\tilde{\sigma}_{\alpha\beta}, \tag{12}$$

where the symmetry property of $\tilde{\sigma}_{\alpha\beta}$ has been used, and the Jacobian, J, is given by

$$J = \left|\frac{\partial X_I}{\partial \xi_\alpha}\right|. \tag{13}$$

It can be further shown that

$$\tilde{\sigma}_{IJ} = \frac{1}{J}F_{I\alpha}F_{J\beta}\tilde{\sigma}^c_{\alpha\beta} - \frac{1}{J}F_{I\alpha}F_{J\beta}\tilde{\sigma}^i_{\alpha\beta} = \tilde{\sigma}^c_{IJ} - \tilde{\sigma}^i_{IJ}. \tag{14}$$

We now consider the equations of motion. In terms of the second Piola-Kirchhoff stress tensor, the equations of motion of the current state, written in the initial configuration, are given by[11]

$$\frac{\partial}{\partial X_J}\left[\tilde{\sigma}^c_{JK}\frac{\partial x_I}{\partial X_K}\right] = \rho^i\frac{\partial^2 u^c_I}{\partial t^2}, \tag{15}$$

where ρ^i is the mass density of the material of the initial state. Making use of (2) and the fact that $\mathbf{u}^i$ is independent of time, we can re-write (15) as

$$\frac{\partial}{\partial X_J}\left[\tilde{\sigma}^c_{JI} + \tilde{\sigma}^c_{JK}\frac{\partial u_I}{\partial X_K}\right] = \frac{\rho}{J}\frac{\partial^2 u_I}{\partial t^2}, \tag{16}$$

where we have used the relationship[11]

$$J = \frac{\rho}{\rho^i}. \tag{17}$$

Furthermore, since the initial state is in static equilibrium, its Cauchy stress σ^i_{IJ} should satisfy

$$\frac{\partial \tilde{\sigma}^i_{JI}}{\partial X_J} = 0. \tag{18}$$

Subtracting (18) from (16) and making use of (14) yields,

$$\frac{\partial}{\partial X_J}\left[\tilde{\sigma}_{JI} + \tilde{\sigma}_{JK}\frac{\partial u_I}{\partial X_K} + \sigma^i_{JK}\frac{\partial u_I}{\partial X_K}\right] = \frac{\rho}{J}\frac{\partial^2 u_I}{\partial t^2}. \tag{19}$$

This is the governing equation for the wave motion u_I superimposed upon the initial state with an existing inelastic strain.

To solve (19), a constitutive relationship between $\widetilde{\sigma}_{IJ}$ and u_I is needed. To this end, consider the Lagrangian strains of the initial and current states (6)–(7). They can be decomposed into elastic and plastic parts,

$$E^i_{\alpha\beta} = E^{ie}_{\alpha\beta} + E^{ip}_{\alpha\beta}, \quad E^c_{\alpha\beta} = E^{ce}_{\alpha\beta} + E^{cp}_{\alpha\beta}. \tag{20}$$

Note that, although the deformation from the natural state to the initial state may involve finite and inelastic strain, $E^{ip}_{\alpha\beta}$, the initial state is in static self-equilibrium. The amplitude of the subsequent ultrasonic wave motion imposed upon the initial state is very small and causes no additional inelastic deformation. Therefore, we must have $E^{ip}_{\alpha\beta} = E^{cp}_{\alpha\beta}$. It thus follows from (8) that the strain difference between the current and initial states is purely elastic, i.e.,

$$E_{\alpha\beta} = E^{ce}_{\alpha\beta} - E^{ie}_{\alpha\beta}. \tag{21}$$

Furthermore, since no additional inelastic strain (plasticity) is induced by the ultrasonic wave motion, the inelastic strain existing in the initial state can be viewed as 'eigenstrain,' so the material can be still considered as elastic in the current state.[13] Therefore, we may introduce a strain energy function W (per unit mass). In an adiabatic and isentropic deformation, the strain energy becomes a function of elastic strain. Thus the strain energy function of the initial and current states can be written, respectively, as

$$\rho W^i = \frac{1}{2} c_{\alpha\beta\gamma\delta} E^{ie}_{\alpha\beta} E^{ie}_{\gamma\delta} + \frac{1}{6} c_{\alpha\beta\gamma\delta\varepsilon\eta} E^{ie}_{\alpha\beta} E^{ie}_{\gamma\delta} E^{ie}_{\varepsilon\eta}, \tag{22}$$

$$\rho W^c = \frac{1}{2} c_{\alpha\beta\gamma\delta} E^{ce}_{\alpha\beta} E^{ce}_{\gamma\delta} + \frac{1}{6} c_{\alpha\beta\gamma\delta\varepsilon\eta} E^{ce}_{\alpha\beta} E^{ce}_{\gamma\delta} E^{ce}_{\varepsilon\eta}, \tag{23}$$

where ρ is the mass density, $c_{\alpha\beta\gamma\delta}$ and $c_{\alpha\beta\gamma\delta\varepsilon\eta}$ are, respectively, the second and third order elastic constants; all of the natural state of the material.

The second Piola-Kirchhoff stress tensors at the initial and current states can be derived from the strain energy functions[11],

$$\tilde{\sigma}^i_{\alpha\beta} = \rho \frac{\partial W^i}{\partial E^{ie}_{\alpha\beta}} = c_{\alpha\beta\gamma\delta} E^{ie}_{\gamma\delta} + \frac{1}{2} c_{\alpha\beta\gamma\delta\varepsilon\eta} E^{ie}_{\gamma\delta} E^{ie}_{\varepsilon\eta}, \tag{24}$$

$$\tilde{\sigma}^c_{\alpha\beta} = \rho \frac{\partial W^c}{\partial E^{ce}_{\alpha\beta}} = c_{\alpha\beta\gamma\delta} E^{ce}_{\gamma\delta} + \frac{1}{2} c_{\alpha\beta\gamma\delta\varepsilon\eta} E^{ce}_{\gamma\delta} E^{ce}_{\varepsilon\eta}. \tag{25}$$

With the help of (21), the above equations lead to

$$\tilde{\sigma}_{\alpha\beta} = \tilde{\sigma}^c_{\alpha\beta} - \tilde{\sigma}^i_{\alpha\beta} = c^0_{\alpha\beta\gamma\delta} E_{\gamma\delta} + \frac{1}{2} c_{\alpha\beta\gamma\delta\varepsilon\eta} E_{\gamma\delta} E_{\varepsilon\eta}, \tag{26}$$

where

$$c^0_{\alpha\beta\gamma\delta} = c_{\alpha\beta\gamma\delta} + c_{\alpha\beta\gamma\delta\varepsilon\eta} E^{ie}_{\varepsilon\eta}. \tag{27}$$

Note that $c^0_{\alpha\beta\gamma\delta}$ has the usual symmetry of elastic constants, i.e.,

$$c^0_{\alpha\beta\gamma\delta} = c^0_{\beta\alpha\gamma\delta} = c^0_{\gamma\delta\alpha\beta}\,. \tag{28}$$

The difference between (27) and a similar equation derived in Pao et al.[10] is that instead of the total strain, only the elastic part of the strain of the initial state appears here. Upon substitution of (9) into (26), we obtain

$$\tilde{\sigma}_{\alpha\beta} = c^0_{\alpha\beta\gamma\delta} A_{\gamma\delta KL} \frac{\partial u_K}{\partial X_L} + \frac{1}{2} c^0_{\alpha\beta\gamma\delta} A_{\gamma\delta JL} \frac{\partial u_K}{\partial X_L} \frac{\partial u_K}{\partial X_J} + \frac{1}{2} c_{\alpha\beta\gamma\delta\varepsilon\eta} A_{\varepsilon\eta KL} A_{\gamma\delta MJ} \frac{\partial u_K}{\partial X_L} \frac{\partial u_M}{\partial X_J}. \tag{29}$$

Making use of (29) in (12) yields the desired constitutive relationship between the stress increment and the ultrasonic wave motion,

$$J\tilde{\sigma}_{IJ} = C_{IJKL} \frac{\partial u_K}{\partial X_L} + \frac{1}{2} D_{IJKLMN} \frac{\partial u_K}{\partial X_L} \frac{\partial u_M}{\partial X_N}. \tag{30}$$

where

$$C_{IJKL} = A_{\alpha\beta IJ} c^0_{\alpha\beta\gamma\delta} A_{\gamma\delta KL}, \tag{31}$$

$$D_{IJKLMN} = A_{\alpha\beta IJ} (c_{\alpha\beta\gamma\delta\varepsilon\eta} A_{\varepsilon\eta KL} A_{\gamma\delta MN} + c^0_{\alpha\beta\gamma\delta} A_{\gamma\delta NL} \delta_{MK}). \tag{32}$$

Because of the symmetries of $c^0_{\alpha\beta\gamma\delta}$ and $A_{\alpha\beta IJ}$, it can be shown that

$$C_{IJKL} = C_{KLIJ} = C_{JIKL}, \tag{33}$$

$$D_{IJKLMN} = D_{JIKLMN} = D_{IJLKMN} = D_{IJKLMN} = D_{IJMNKL}\,. \tag{34}$$

Finally, substituting (30) into (19) yields

$$\frac{\partial}{\partial X_J}\left[\frac{1}{J}\left(C_{IJKL} + J\sigma^i_{JL}\delta_{IK} + \left(C_{JLMN}\delta_{IK} + \frac{1}{2} D_{IJKLMN}\right)\frac{\partial u_M}{\partial X_N}\right)\frac{\partial u_K}{\partial X_L}\right] = \frac{\rho}{J}\frac{\partial^2 u_I}{\partial t^2} \tag{35}$$

3. ACOUSTIC NONLINEARITY PARAMETER OF ANISOTROPIC MATERIALS

In anisotropic materials, the ultrasonic waves do not necessarily propagate in pure longitudinal or shear modes. The nonlinearity parameter for such

quasi-modes in an anisotropic material can be defined in a way similar to Breazeale and Philip[14] and Cantrell[15]. Without loss of generality, we choose the 1-direction as the propagation direction. Furthermore, we assume that the inelastic deformation of the initial state is uniform, i.e., $F_{I\alpha}$ is constant throughout the domain of interest. Equation (35) can then be written as

$$\left(C^{(1)}_{IK} + D^{(1)}_{IKM}\frac{\partial u_M}{\partial X_1}\right)\frac{\partial^2 u_K}{\partial X_1 \partial X_1} = \rho\frac{\partial^2 u_I}{\partial t^2}, \tag{36}$$

where

$$C^{(1)}_{IK} = C_{I1K1} + J\sigma'_{11}\delta_{IK},$$
$$D^{(1)}_{IKM} = 2C_{11M1}\delta_{IK} + D_{I1K1M1}. \tag{37}$$

Because of the diagonal symmetry of C_{IJKL}, it is easy to see that $C^{(1)}_{IK}$ is also symmetric.

For a plane wave propagating in the 1-direction, we may write

$$u_I = U_I e^{ik(X_1 - ct)}, \tag{38}$$

where k is the wavenumber and c is the phase velocity. Inserting (38) into (36) and neglecting nonlinear terms for now, we obtain the Christoffel equation,

$$\left[C^{(1)}_{IK} - \rho c^2 \delta_{IK}\right]U_K = 0. \tag{39}$$

Since $C^{(1)}_{IK}$ is symmetric, there exist three real eigenvalues $\lambda_{(n)}$ and three real eigenvectors (i.e. polarization vectors), $\mathbf{U}^{(n)}$. A transformation matrix $\mathbf{P}$ can then be constructed by placing the three real eigenvectors side by side

$$\mathbf{P} = [\mathbf{U}^{(1)}\mathbf{U}^{(2)}\mathbf{U}^{(3)}]. \tag{40}$$

Then, we have from (39) that

$$P_{I(n)}C^{(1)}_{IJ}P_{J(n)} = \lambda_{(n)} \quad \text{for } n = 1, 2, 3 \tag{41}$$

Note that indices with parentheses are not summed.

Next, we let

$$u_I = P_{IJ}u^{(P)}_J \,. \tag{42}$$

Then, substitution of (42) into (36) in conjunction with (41) yields,

$$\rho^i \frac{\partial^2 u^{(P)}_I}{\partial t^2} = \lambda_{(I)}\frac{\partial^2 u^{(P)}_I}{\partial X_1^2} + \Lambda_{IJK}\frac{\partial u^{(P)}_J}{\partial X_1}\frac{\partial^2 u^{(P)}_K}{\partial X_1^2}, \tag{43}$$

where

$$\Lambda_{IJK} = P_{I'I}D^{(1)}_{I'J'K'}P_{JJ'}P_{KK'} \,. \tag{44}$$

It has been shown[16] that the off-diagonal terms in Λ_{IJK} (representing the coupling between modes) are several orders of magnitude smaller than the diagonal terms 1(unimodal terms). So, by neglecting the off-diagonal terms in Λ_{IJK}, equation (43) can be written as,

$$\frac{\partial^2 u^{(P)}_I}{\partial t^2} = c_I^2\left(1 + \frac{\Lambda_{(I)(I)(I)}}{\lambda_{(I)}}\frac{\partial u^{(P)}_{(I)}}{\partial X_1}\right)\frac{\partial^2 u^{(P)}_{(I)}}{\partial X_1^2} \,. \tag{45}$$

Therefore, the nonlinearity parameter for wave mode, I, propagating in 1-direction is defined as

$$\beta_I = -\frac{\Lambda_{(I)(I)(I)}}{\lambda_{(I)}} \,. \tag{46}$$

4. EXAMPLES AND DISCUSSIONS

As an example to illustrate the formation developed above, we consider the deformation of the FCC single crystal copper under cyclic fatigue. The fatigue behavior of copper single crystals has been investigated extensively by Mughrabi[17] and Mughrabi et al.[18] An extensive review and discussion on the cyclic deformation of FCC single crystals is found in Reference 19. The displacement gradient tensor in (3) is calculated from the plastic strain amplitude available in the literature.[17,18]

A specimen oriented for single slip to occur in the (111) plane along the [101] direction was fatigued by a fully reversed cyclic loading in the [123] direction with a fixed plastic shear strain amplitude γ_{pl}. The specimens were fatigued until saturation states were attained. Figure 2 schematically shows the

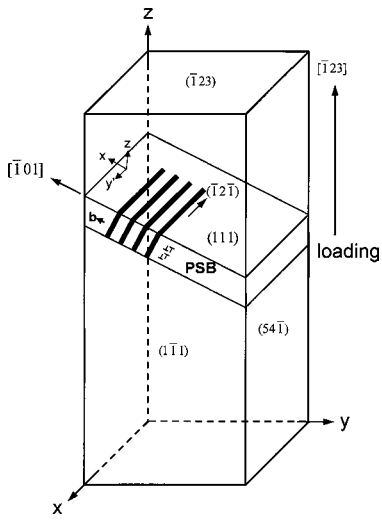

Fig. 2. Schematic showing orientations of sample faces, slip place, and loading direction.

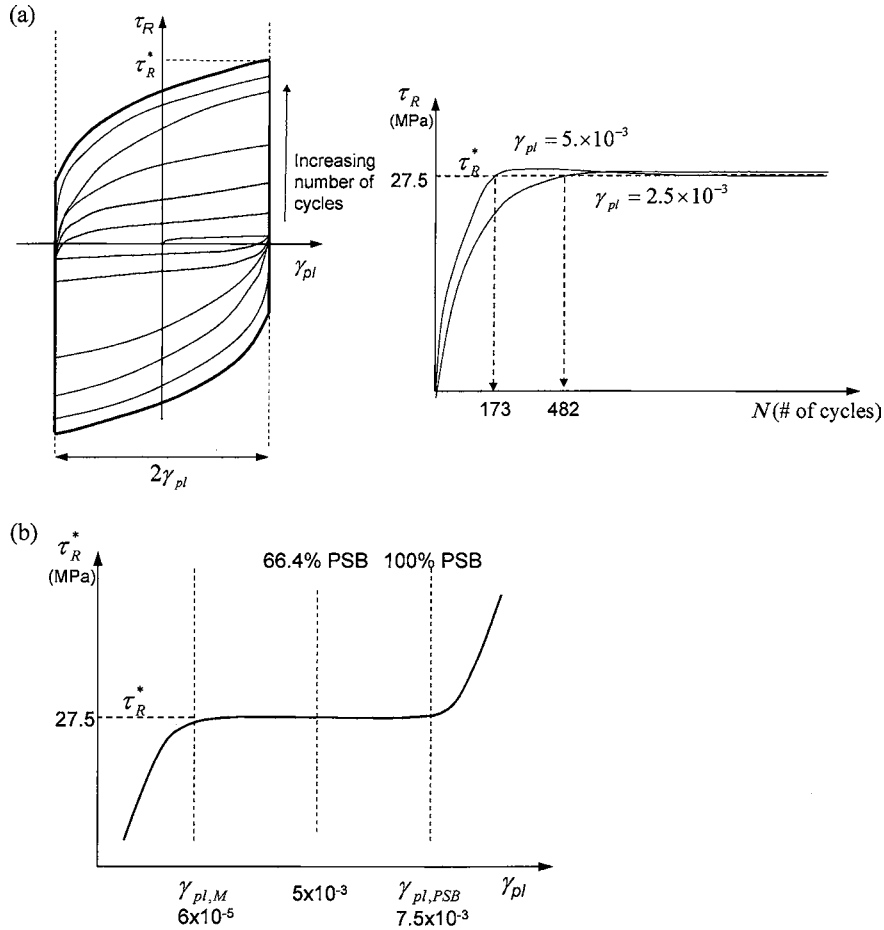

Fig. 3. Cyclic hardening and saturation behavior of a single crystal copper fatigued at a fixed resolved plastic strain (γ_{pl}). (a) Resolved shear stress (τ_R) vs. resolved plastic strain, (b) Saturation stress vs. resolved plastic strain.

relative directions of the loading, slip plane and specimen faces. It is characteristic of FCC single crystals that cyclic loading produces strain-localization zones called persistent slip bands (PSBs). PSBs are the dislocation substructure characterized by a ladder-like regular arrangement of dislocation-rich walls and dislocation-poor channels. Higher dislocation density in the walls leads to high deformability of the PSBs, which thus can carry most of the plastic strain in the specimen. It has been observed that a saturated state is attained after a rapid initial cyclic hardening as shown in Fig. 3(a). In the saturated state, the volume fraction of PSBs measured by their surface markings remains unchanged for a fixed plastic resolved strain amplitude and temperature. Due to the saturation of PSB volume fraction, the resolved shear stress or the flow stress saturates as well, exhibiting a constant hysteresis loop (Fig. 3(a)). Another consequence of the saturation is the plateau region in the cyclic stress-strain curve (CSSC) as shown in Fig. 3(b). In Fig. 3(b), the lower and upper extremes of the plateau of the CSSC are known to correspond to the plastic strain amplitudes that can be accommodated by the matrix ($\gamma_{pl,M}$) and by the PSBs ($\gamma_{pl,PSB}$) in the saturation state. The plastic shear strains at extremes of the plateau regime were measured as $\gamma_{pl,M} = 6 \times 10^{-5}$ and $\gamma_{pl,PSB} = 7.5 \times 10^{-3}$. The volume fraction of PSBs between $\gamma_{pl,M}$ and $\gamma_{pl,PSB}$ were observed[17] to increase linearly with the plastic strain amplitude, that is,

$$f_{PSB} = (\gamma_{pl} - \gamma_{pl,M}) / (\gamma_{pl,PSB} - \gamma_{pl,M}),$$
$$\gamma_{pl,M} \leq \gamma_{pl} \leq \gamma_{pl,PSB}. \quad (47)$$

The plastic shear amplitudes selected for our calculations are $\gamma_{pl} = 2.5 \times 10^{-3}$ and 5×10^{-3}. The total cumulative plastic shear strains are 24.8 and 26.48, which correspond to numbers of cycles of 2480 and 1324, respectively. The saturations occurred at cumulative plastic shear strains about 4.28 and 3.46. These are obtained from Fig. 1 of Mughrabi.[17] It is assumed that the volume fraction of PSBs before saturation increases linearly with the number of fatigue cycles. The volume fractions of PSBs at saturation according to (47) are 32.8 % and 66.4 %.

The residual shear stress in the specimen is estimated using the information available in Mughrabi[17] and Mughrabi et al.[18] and based on a simple consideration of the microstructure. The residual stress is regarded as the average shear stress in the specimen produced by the plastic shear strain. Since the PSBs in FCC crystals are formed as bulk layers traversing throughout the whole cross section of the specimen (rather than as isolated inclusions), the overall stress can be estimated approximately by the rule of mixtures as

$$\tau^{res} = (1 - f_{PSB})\tau^{M} + f_{PSB}\tau^{PSB}, \qquad (48)$$

where τ^{M} and τ^{PSB} are the shear stresses in the matrix and PSBs at the saturation state. The shear stress in the PSB was measured as $\tau^{PSB} = 27.5$ MPa for copper single crystals at room temperature[17,18] and that in the matrix may be calculated by

$$\tau^{M} = \gamma_{pl,M} G = \gamma_{pl,M}[C_{44}(C_{11} - C_{12})/2]^{1/2} \approx 2.5 \text{ kPa}.$$

From these values, the saturated residual shear stresses for $\gamma_{pl} = 2.5 \times 10^{-3}$ and 5×10^{-3} are about 9 MPa and 18.3 MPa, respectively. Figure 4 shows

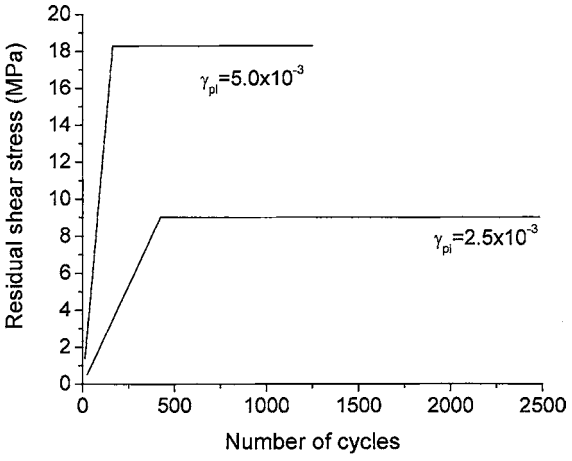

Fig. 4. Residual stress change during fatigue for two different plastic strain amplitudes.

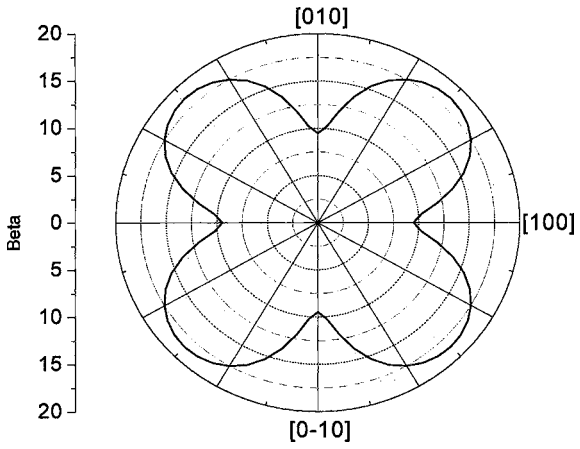

Fig. 5. Orientation dependence of acoustic nonlineairy parameter in cubic copper.

the residual stress vs. number of fatigue cycles. The second order elastic constants of single crystal copper used for the calculations are $C_{11} = 168.4$, $C_{12} = 121.4$, $C_{44} = 75.4$ in GPa and the third order elastic constants $C_{111} = -1271$, $C_{112} = -814$, $C_{123} = -50$, $C_{144} = -3$, $C_{166} = -780$, $C_{456} = -95$ in GPa. The density is 8920 kg/m^3.

Figure 5 shows the orientation dependence of the acoustic nonlinearity parameter β of a longitudinal wave in the (001) plane of the cubic copper before fatigue, calculated numerically using Eq. (46) with the plastic strain and residual set to be zero. An explicit functional form of Eq. (46) in terms of the second and third order elastic constants exists only for propagations in the axial, face-diagonal, and body-diagonal directions.[15] It is assumed that the cubic copper is a perfect crystal that has no atomic defects. Therefore, the figure shows the intrinsic material lattice anharmonicity.[14] It is seen that the acoustic nonlinearity due to the lattice anharmonicity is in the range of $10 \sim 18$, which is the range of the initial acoustic nonlinearity. It is noted that the acoustic nonlinearity has an angular dependence similar to the longitudinal wave speed: both are maximal in the face-diagonal directions ($[\pm 1/\sqrt{2}, \pm 1/\sqrt{2}, 0]$).

Figures 6 and 7 show the longitudinal wave acoustic nonlinearity parameters of the copper single crystal as a function of the number of fatigue cycles, for two different plastic strain amplitudes ($\gamma_{pl} = 2.5 \times 10^{-3}$ and 5×10^{-3}). The three different curves correspond to three different propagation directions of the longitudinal wave (propagation in the X, Y, and Z directions in Fig. 2). The acoustic nonlinearity parameter is observed to increase

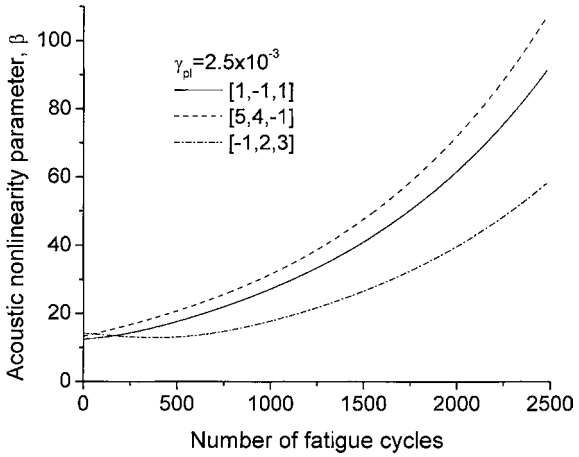

Fig. 6. Acoustic nonlinearity parameter during fatigue for resolved plastic strain amplitude of 2.5×10^{-3}.

monotonically by a significant amount. The increase is slightly more pronounced for higher plastic strain amplitude ($\gamma_{pl} = 5.0 \times 10^{-3}$). This may be explained by considering the failure mode in the fatigued single crystal. The crystal can be deformed in a single deformation mode (the primary slip, assuming that the cross slips are small) without any constraint, and thus the plastic strain as well as the dislocation density increases continuously until its failure; so does the acoustic nonlinearity. It is important to note that this failure behavior would be much different in polycrystalline materials; such high plastic strain does not occur in polycrystalline materials, since the plastic deformation in each grain is constrained by surrounding grains. The accumulation of local plastic strain at the grain boundaries may lead to crack initiation. This crack initiation causes a stress concentration at that site, while it relaxes stress in other parts of the material, which results in retardation of global plastic deformation. For this reason, the plasticity induced acoustic nonlinearity in polycrystalline materials should tend to saturate with crack initiation. Therefore, the present results in copper single crystals serve as the upper bounds of the acoustic nonlinearity of polycrystalline coppers under similar fatigue conditions.

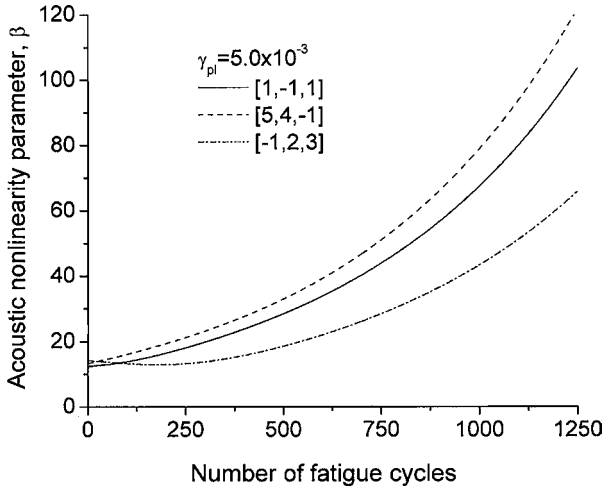

Fig. 7. Acoustic nonlinearity parameter during fatigue for resolved plastic strain amplitude of 5.0×10^{-3}.

In our calculations, the acoustic nonlinearity parameter of the entire specimen was predicted using the applied resolved plastic shear strain amplitude, which is the average plastic shear strain from the specimen, as the input parameter. For this reason, the predicted acoustic nonlinearity parameters may be close to those in the PSBs, e.g., the local microplasticity, since the entire material volume is assumed to have the same plastic shear strain. For a more accurate prediction of the overall nonlinearity parameter, a micromechanical averaging scheme needs to be applied. The present model seems also to predict a significant change in the second order elastic constants, which results in a significant change in linear acoustic properties such as the phase velocity, although significant changes of phase velocity in fatigue samples has not been observed experimentally. The reason for this is not clear and is currently under investigation. It is noted that a similar change in the second order elastic constants is also predicted by other models[9] for calculating the acoustic nonlinearity of fatigued materials.

5. SUMMARY

Since the nonlinear ultrasonic technique has been found to be successful in experimentally evaluating fatigue damage in different materials, an analytical model is needed that quantitatively relates the measured acoustic nonlinearity parameter to the damage state of the material. The model developed here provides a direct and quantitative link between the acoustic nonlinearity parameter and the cumulative plastic strain in the fatigued sample. In conjunction with fatigue models that relate the cumulative plastic strain to fatigue life, the model developed here can be used to nondestructively evaluate the remaining fatigue life of a sample by measuring the acoustic nonlinear parameter.

It is important to note that acoustic nonlinearity can be caused by a number of different sources. The present model considers the contribution from residual microplasticity only. An advantage of the present model is that it is formulated in terms of cumulative plastic strain, rather than dislocation density. This enables us to directly utilize existing models for crystal plasticity and experimental observations of fatigue damage.

ACKNOWLEDGEMENTS

This work is supported by the Defense Advanced Projects Agency (DARPA), Defense Sciences Office (DSO), Engine Systems Prognosis, under a subcontract to Prime Contract No. HR0011-04-C-0001 and is approved for public release, distribution unlimited.

REFERENCES

1. R. Truell, C. Elbaum, and B. B. Chick, *Ultrasonic Methods in Solid State Physics* (Academic Press, New York., 1969).
2. T. Suzuki, A. Hikata, and C. Elbaum, Anharmonicity due to glide motion of dislocations, *J. Appl. Phys.* **35**, pp. 2761 (1964).
3. A. Hikata, B. B. Chick, and C. Elbaum, Dislocation contribution to the second harmonic generation of ultrasonic waves, *J. Appl. Phys.* **36**, pp. 229 (1965).
4. P. B. Nagy, Ultrasonics Fatigue damage assessment by nonlinear ultrasonic materials characterization, **36**, pp. 375 (1998).
5. W. L. Morris, O. Buck, and R. V. Inman, Acoustic harmonic generation due to fatigue damage in high-strength aluminum, *J. Appl. Phys.* **50**, pp. 6737 (1979).
6. A. V. Granato and K. Lucke, Theory of mechanical damping due to dislocations, *J. Appl. Phys.* **27**, pp. 583 (1956).
7. J. H. Cantrell and W. T. Yost, Acoustic harmonic generation from fatigue-induced dislocation dipoles, *Philos. Mag.* **A69**, pp. 315 (1994).
8. J. H. Cantrell, Substructural organization, dislocation plasticity and harmonic generation in cyclically stressed wavy slip metals, *Proc. Roy. Soc. Lond. A* **460**, pp. 757 (2004).
9. J. H. Cantrell, Quantitative assessment of fatigue damage accumulation in wavy slip metals from acoustic harmonic generation, *Philos. Mag.* to appear (2005).
10. Y.-H. Pao, W. Sachse, and H. Fukuoka, *Physical Acoustics* (Academic Press, 1984, vol. 17, pp. 61).
11. L. Malvern, *Introduction to the Mechanics of a Continuous Medium.* (Prentice-Hall, Inc., Englewood, New Jersey, 1969).
12. A. E. Green and J. E. Adkins, *Large Elastic Deformations*, 2nd ed. (Oxford University Press, Oxford, 1970).
13. T. Mura, *Micromechanics of Defects in Solids* (Martinus Nijhoff Pub., Boston, MA., 1987).
14. M. A. Breazeale and J. Philip, *Physical acoustics* (1984, vol. 17, pp. 1).
15. J. H. Cantrell, Crystalline structure and symmetry dependence of acounstic nonlinearity parameters, *J. Appl. Phys.* **76**, pp. 3372 (1994).
16. A. C. Holt and J. Ford, Theory of ultrasonic pulse measurements of third-order elastic constants for cubic crystals, *J. Appl. Phys.* **38**, pp. 42 (1967).
17. H. Mughrabi, The cyclic hardening and saturation behavior of copper single crystals, *Mater. Sci. Eng.* **33**, pp. 207 (1978).
18. H. Mughrabi, F. Ackerman, and K. Herz, *Fatigue Mechanisms, edited by Special Technical Publication* (ASTM, Special Technical Publication, Philadelphia, 1979, vol. 675, pp. 69).
19. S. Suresh, *Fatigue of Materials*, 2nd ed. (Cambridge University Press, New York, 1998).